UNIVERSITÉ DE GENÈVE

Archive ouverte UNIGE
https://archive-ouverte.unige.ch

Article scientifique | Article | 2022

Published version | Open Access

This is the published version of the publication, made available in accordance with the publisher's policy.

Physiologically variable ventilation prevents lung function deterioration in a model of pulmonary fibrosis

Dos Santos Rocha, André Alexandre; Petak, Ferenc; Carvalho, Tânia; Habre, Walid; Balogh, Adam Laszlo

How to cite

DOS SANTOS ROCHA, André Alexandre et al. Physiologically variable ventilation prevents lung function deterioration in a model of pulmonary fibrosis. In: Journal of applied physiology, 2022, vol. 132, n° 4, p. 915–924. doi: 10.1152/japplphysiol.00670.2021

This publication URL: https://archive-ouverte.unige.ch/unige:170433
Publication DOI: 10.1152/japplphysiol.00670.2021

© This document is protected by copyright. Please refer to copyright holder(s) for terms of use.

american physiological society

JOURNAL OF APPLIED PHYSIOLOGY

J Appl Physiol 132: 915–924, 2022.
First published February 24, 2022; doi:10.1152/japplphysiol.00670.2021

RESEARCH ARTICLE

Physiologically variable ventilation prevents lung function deterioration in a model of pulmonary fibrosis

André Dos Santos Rocha,[1] Ferenc Peták,[2] Tânia Carvalho,[3] Walid Habre,[1,4] and Adam L. Balogh[1]

[1]*Unit for Anaesthesiological Investigations, Department of Acute Medicine, University Hospitals of Geneva and University of Geneva, Geneva, Switzerland;* [2]*Department of Medical Physics and Informatics, University of Szeged, Szeged, Hungary;* [3]*Histology and Comparative Pathology Laboratory, Instituto de Medicina Molecular, Lisbon, Portugal; and* [4]*Pediatric Anesthesia Unit, Geneva Children's Hospital, Geneva, Switzerland*

Abstract

Positive pressure ventilation exerts an increased stress and strain in the presence of pulmonary fibrosis. Thus, ventilation strategies that avoid high pressures while maintaining lung aeration are of paramount importance. Although physiologically variable ventilation (PVV) has proven beneficial in various models of pulmonary disease, its potential advantages in pulmonary fibrosis have not been investigated. Therefore, we assessed the benefit of PVV over conventional pressure-controlled ventilation (PCV) in a model of pulmonary fibrosis. Lung fibrosis was induced with intratracheal bleomycin in rabbits. Fifty days later, the animals were randomized to receive 6 h of either PCV (n = 10) or PVV (n = 11). The PVV pattern was prerecorded in spontaneously breathing, healthy rabbits. Respiratory mechanics and gas exchange were assessed hourly; end-expiratory lung volume and intrapulmonary shunt fraction were measured at *hours 0* and *6*. Histological and cellular analyses were performed. Fifty days after bleomycin treatment, the rabbits presented elevated specific airway resistance [69 ± 26% (mean ± 95% confidence interval)], specific tissue damping (38 ± 15%), and specific elastance (47 ± 16%) along with histological evidence of fibrosis. Six hours of PCV led to increased respiratory airway resistance (Raw, 111 ± 30%), tissue damping (G, 36 ± 13%) and elastance (H, 58 ± 14%), and decreased end-expiratory lung volume (EELV, −26 ± 7%) and oxygenation (Pa_{O_2}/FI_{O_2}, −14 ± 5%). The time-matched changes in the PVV group were significantly lower for G (22 ± 9%), H (41 ± 6%), EELV (−13 ± 6%), and Pa_{O_2}/FI_{O_2} ratio (−3 ± 5%, $P < 0.05$ for all). There was no difference in histopathology between the ventilation modes. Thus, prolonged application of PVV prevented the deterioration of gas exchange by reducing atelectasis development in bleomycin-induced lung fibrosis.

NEW & NOTEWORTHY The superposition of physiological breathing variability onto a conventional pressure signal during prolonged mechanical ventilation prevents atelectasis development in bleomycin-induced lung fibrosis. This advantage is evidenced by reduced deterioration in tissue mechanics, end-expiratory lung volume, ventilation homogeneity, and gas exchange.

atelectasis; bleomycin; functional residual capacity; lung fibrosis; mechanical ventilation

INTRODUCTION

Recently, there has been increasing interest in mechanical ventilation modes that mimic physiological respiration. Most experimental and clinical studies have shown that the introduction of a certain degree of variability in the tidal volume (V_T), i.e., the amplitude of ventilation, is beneficial for both gas exchange and respiratory mechanics (1–5). Furthermore, our research group has recently developed a ventilation modality based on a prerecorded physiological spontaneous breathing pattern. Introduction of physiological variability prevented the deleterious consequences on lung function induced by prolonged monotonous positive pressure ventilation, both in healthy (6) and injured lungs (7).

The benefits of variable ventilation are due to improved recruitment of alveolar units, enhanced surfactant production, and preservation of gas exchange (1, 3, 8–11), which was also manifested in preserved alveolar structure reflected by maintained lung compliance (2, 4, 5, 12) and by lower lung histological injury scores (6). The advantage of variable ventilation has been established in models of asthma (13), chronic obstructive lung disease (COPD) (14), and acute respiratory distress syndrome (ARDS) (3, 15–17). Nevertheless, the effects of variability on ventilator-induced deterioration in lung function have not been investigated in the presence of chronic fibrosis in the lung parenchyma.

In the present study, the potential benefit of physiologically variable ventilation (PVV) over conventional pressure-controlled ventilation (PCV) was assessed in a well-validated animal model of pulmonary fibrosis (18–21). The importance of this study lies within the notion that under linear pressure-volume relationship a unit strain generates greater stress in interstitial lung diseases than in healthy lungs or

Correspondence: A. Dos Santos Rocha (Andre.DosSantosRocha@unige.ch).
Submitted 22 September 2021 / Revised 26 January 2022 / Accepted 20 February 2022

8750-7587/22 Copyright © 2022 the American Physiological Society.

Downloaded from journals.physiology.org/journal/jappl at Univ De Geneve (129.194.001.044) on November 15, 2022.

even the "baby lung" in ARDS (22), thus making it more susceptible to ventilation-induced lung injury (23). Therefore, we hypothesized that PVV is potentially less injurious and prevents lung function deterioration in an animal model of pulmonary fibrosis.

METHODS

Ethical Statement

Approval from the Animal Welfare Committee of the Canton of Geneva and the Experimental Ethics Committee of the University of Geneva, Switzerland, was obtained (no. GE 12/20, 10 February 2020). During the experiments, the current animal protection laws of Switzerland were followed (LPA, RS455). The current study is reported in accordance with the ARRIVE guidelines.

Experimental Animals

Fourteen-week old New Zealand White rabbits of both sexes (13 males and 9 females) were purchased from the farm of University of Geneva (Arare, Geneva, Switzerland) and were delivered at least 2 days before the experiments to allow acclimatization. Food and water were supplied to the rabbits ad libitum before the experiments.

Anesthesia and Induction of Pulmonary Fibrosis on *Day 0*

Anesthesia was induced with an intramuscular injection of ketamine (25 mg/kg) and xylazine (3 mg/kg). After an ear vein had been cannulated, topical anesthesia with 10% lidocaine was applied in the larynx, and a 3.0-mm inner diameter (ID) cuffed endotracheal tube was inserted. Subsequently, anesthesia was maintained with intravenous remifentanil (100 μg/kg/h). Mechanical ventilation was then started in volume-controlled mode with a V_T of 7 mL/kg. Respiratory rate was adjusted to maintain the end-tidal CO_2 value in the normal range.

Pulmonary fibrosis was induced by adopting a well-established approach based on the intratracheal administration bleomycin (1.8 U/kg dissolved in 1 mL saline 0.9%) (18, 20, 21) using a vibrating mesh aerosolizer (Aerogen Solo Nebulizer System, Hamilton Medical, Switzerland). The animals were awakened and subsequently assessed daily using a welfare score until *day 50*.

Anesthesia and Surgical Preparation on *Day 50*

Anesthesia was induced in a manner identical to *day 0* (ketamine, xylazine). Maintenance of anesthesia was provided by continuous intravenous propofol (10 mg/kg/h), fentanyl (5 μg/kg/h), and midazolam (0.2 mg/kg/h) through a 24 G catheter (Abbocath, Abbot Medical, Baar/Zug, Switzerland) inserted in the ear vein. A rectal probe was used to monitor body temperature, which was kept within the 38°C–39°C range using a thermostatic heating pad (Harvard Apparatus, South Natick, MA). The anterior cervical region was infiltrated with lidocaine 1% (Sintetica, Mendrisio, Switzerland), and a 3.5-mm uncuffed tube (3.5 mm Portex, Smiths Medical, Kent, UK) was inserted into the trachea via a tracheostomy. After ensuring an appropriate anesthesia depth, neuromuscular blockade was maintained with intravenous atracurium (0.6 mg/kg/h). The left femoral artery and the right jugular vein were cannulated with 20 G catheters (Abbocath, Abbot Medical, Baar/Zug, Switzerland) for blood sampling. Arterial, central venous and airway opening pressures, electrocardiogram, and body temperature were continuously monitored throughout the study period (ADInstruments, Powerlab model 8/35, and LabChart 7, Dunedin, New Zealand). Driving pressure ($P_{driving}$) was calculated as the difference between positive end-expiratory pressure (PEEP) and peak inspiratory pressure.

Multiple-Breath Helium Washout Technique

The multiple-breath washout (MBW) technique with helium as tracer gas was used to measure end-expiratory lung volume (EELV) (24). An ultrasonic flowmeter (Spiroson Scientific; ECO Medics AG, Dürnten, Switzerland) placed between the endotracheal tube connector and the ventilator circuit was used to measure signals of flow and molar mass whereas helium was washed in to the ventilatory circuit during several breaths until it reached a steady-state end-inspiratory concentration of 4%–5%. The MBW curve was subsequently recorded after interrupting the administration of helium; this washout phase was used to calculate EELV using a computer algorithm (Spiroware V1.4.3). The lung clearance index (LCI) was determined as previously described (25, 26), as the number of turnovers required to decrease the end-tidal helium concentration to 1/40th of the initial value before washout.

Measurement of Respiratory Mechanical Parameters

Respiratory mechanical parameters were assessed by the wave-tube method for the forced oscillation technique, as described previously (27). The airway and tissue compartments of the respiratory system were separated by fitting a well-validated model (28) to the obtained spectra. The model consists of an airway compartment with a resistive (Raw, airway resistance) and an inertive (Iaw, airway inertance) component in series with a constant-phase tissue compartment including tissue damping (G) and tissue elastance (H). As previously shown (29), Raw reflects the flow resistance of the central airways, Iaw relates to the acceleration and deceleration of air in the central airways, G characterizes the energy loss in the respiratory tissues, and H describes the energy storage properties of the tissues (elastance). The impedance of the instrumental apparatus was measured and subtracted from the Zrs spectra. At each protocol stage, four data epochs were collected in 1-min intervals and ensemble averaged for model fitting. To eliminate the effects of altered lung volume subsequent to lung growth and bleomycin treatment, the changes in respiratory mechanical parameters between *day 0* and *day 50* were expressed as specific Raw (sRaw = Raw · EELV), specific G (sG = G · EELV), and specific H (sH = H · EELV).

Blood Analyses

Partial pressure of oxygen and carbon dioxide in the arterial (Pa_{O_2}, Pa_{CO_2}) and central venous (Pv_{O_2},Pv_{CO_2}) blood were measured by using a point-of-care blood gas analyzer (i-Stat, Abbott Laboratories, Chicago, IL). Oxygenation index was

Downloaded from journals.physiology.org/journal/jappl at Univ De Geneve (129.194.001.044) on November 15, 2022.

calculated as Pa_{O_2} divided by the fraction of inspired oxygen (FI_{O_2}). The intrapulmonary shunt fraction was calculated using the Berggren equation as $(Ca_{O_2} - Cc_{O_2})/(Cv_{O_2} - Cc_{O_2})$, where Ca_{O_2}, Cv_{O_2}, and Cc_{O_2} are the oxygen contents of the arterial, venous and pulmonary capillary blood, respectively (30).

Physiologically Variable Ventilation Pattern

The PVV pattern was based on a recording from spontaneously breathing healthy rabbits, using whole body plethysmography; the characteristics of the PVV pattern were described previously (31). The PVV pattern was applied via a commercial neonatal ventilator (Servo-i, Maquet Critical Care, Solna, Sweden) with special firmware, using custom-made computer software.

Bronchoalveolar Lavage

The cell content of the bronchoalveolar lavage fluid (BALF) was analyzed as described previously (6). Briefly, the BALF was centrifuged at 412 *g* for 5 min at 5°C. The cell pellet was resuspended in phosphate-buffered saline with bovine serum albumin and cytospin preparations were obtained by centrifugation at 58 *g* for 7 min. For differential cell counting, the fixed and stained (May–Grünwald–Giemsa) slides were scanned using Mirax Scan (Carl Zeiss MicroImaging, Jena, Germany). Cells were counted using image acquisition software (Panoramic viewer, 3DHISTECH Ltd, Budapest, Hungary). Four hundred cells were randomly counted in each cytospin preparation, and the percentual number was obtained by differential cell count.

Lung Histopathology

The left lung was filled through the main bronchi at a hydrostatic pressure of 20 cmH_2O with formaldehyde (4%). The formalin-fixed left lung was grossly sectioned at six levels (5-mm slices spaced by 5 mm), embedded in paraffin, and serially sectioned at 4 μm for staining with hematoxylin and eosin and Masson's trichrome. Histological analysis was performed by a pathologist blinded to experimental groups. To assess severity and the extension of lung fibrosis, 20 histological fields (×200) of the left lung lobes were analyzed using a semiquantitative grading system as described previously (32, 33). Areas with dominating tracheal or bronchial tissue were omitted. To assess severity and extension of alveolar damage, we used a semiquantitative grading system in accordance with American Thoracic Society guidelines (34), considering the presence of polymorphonuclear cells in the alveolar and interstitial spaces, hyaline membranes, proteinaceous debris filling the airspaces, and alveolar septal thickening. Briefly, 20 random histological fields (×400) of the left lung lobes were analyzed, and the overall histological injury score was calculated by averaging the score of each lung field.

Experimental Protocol

The scheme of the experimental protocol is depicted in Fig. 1. After surgical preparation on *day 50*, the animals were randomized into Group PCV (n = 10) or Group PVV (n = 11). After establishing stable hemodynamic and respiratory conditions, two deep inflations (25 cmH_2O peak pressure maintained for 10 s each) were applied to normalize lung volume history. All rabbits were initially ventilated in PCV mode with a target V_T of 7 mL/kg and a PEEP of 3 cmH_2O. A set of measurements was performed to establish the baseline values of forced oscillatory respiratory mechanics, blood gases, EELV, and LCI (*H0*). Ventilation in pressure-controlled mode was continued for the rabbits of the PCV group, whereas variable ventilation was initiated for the animals of the PVV group. The amplitude of the inspiratory pressure was adapted in both groups throughout the 6-h ventilation period to maintain a mean V_T of 7 mL/kg, whereas normocapnia was ensured by adjusting the respiratory rate. A fixed inspiratory-to-expiratory time ratio of 1:2 was used. Arterial blood gas and a set of forced oscillation data were collected hourly for the following 5 h (*H1–H5*). The same set of data collected at *H0* was collected after 6 h (*H6*). On *day 0*, at *H0* and *H6*, forced oscillatory and MBW measurements were also performed at a PEEP of 6 cmH_2O. Animals were euthanized

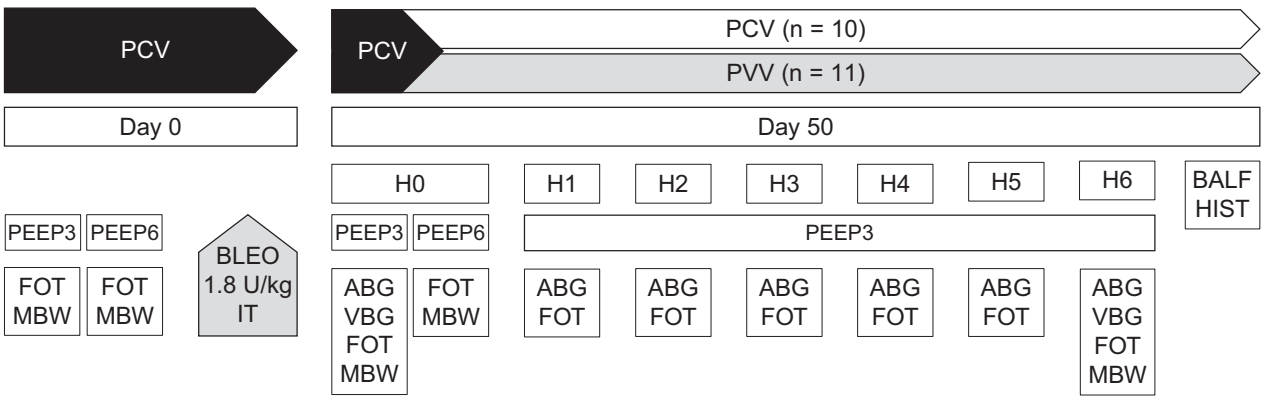

Figure 1. Scheme of the experimental protocol. Pulmonary fibrosis was induced via intratracheal nebulization of 1.8 U/kg bleomycin (BLEO) on *day 0*. Respiratory mechanics using the forced oscillation technique (FOT) and end-expiratory lung volume (EELV) using multiple-breath helium washout tests (MBW) were measured before bleomycin treatment at 3 and 6 cmH_2O positive end-expiratory pressure (PEEP). On *day 50*, the rabbits underwent mechanical ventilation with either pressure-controlled mode (Group PCV), or physiological variable ventilation (Group PVV). Forced oscillatory measurements and arterial blood gas analyses (ABG) were performed hourly. At *H0* and *H6*, additional MBW measurements and venous blood gas analyses (VBG) were performed. *n*, Number of animals. BALF, bronchoalveolar lavage fluid; HIST, histological analysis.

Downloaded from journals.physiology.org/journal/jappl at Univ De Geneve (129.194.001.044) on November 15, 2022.

by injecting a single intravenous dose of pentobarbital (50 mg/kg). Bronchoalveolar lavage was performed ex vivo in the right lung, and the left lung was extracted for histological analyses.

Statistical Methods

We estimated the sample size based on an H that was previously obtained under similar experimental conditions in rabbits (6). We aimed at detecting 25% between-group differences, assuming an interindividual variation of 15%, a statistical power of 0.8, and a two-sided alpha error of 0.05. The calculation resulted in a sample size of 11 rabbits per group. Accordingly, we involved 22 rabbits in the experiment. One animal did not survive the intubation procedure before the bleomycin treatment.

Data are presented as mean (95% confidence interval) unless otherwise specified. Normality of the data was assessed for each variable using the Shapiro–Wilk test. Three-way repeated analyses of variances (ANOVA) were used to compare the absolute values of specific respiratory mechanical parameters (sRaw, sG, and sH), with group allocation (PCV or PVV) as between-subject and PEEP (3 vs. 6 cmH_2O) and time (*D0* vs. *H0*) as within-subject factors. The absolute values of the other respiratory parameters were compared by applying two-way repeated measures ANOVA, using group allocation as between-subject and time (*H0* to *H6*) as within-subject factors. In case of significance, pairwise comparisons were performed using Student's *t* test with Holm–Sidak correction with Group PCV and *H0* as reference values. Relative changes in all parameters between *H0* and *H6* were analyzed using an unpaired *t* test or a Mann–Whitney test, depending on normality. The statistical tests were performed using SigmaPlot (version 13, Systat Software, Inc., Chicago, IL) and the *lme4* (35) and *emmeans* (36) packages in the R environment. Results were considered significant for a level of $P < 0.05$, and all *P* values are two sided.

RESULTS

There was no significant difference in body weight between the protocol groups. The mean body weight of the animals increased from 2.98 kg (2.87–3.09 kg) on *day 0* to 3.61 kg (3.47–3.74 kg) on *day 50*. All subsets of data analyzed with two-way or three-way ANOVA passed the Shapiro–Wilk test for normality.

Uniform increases in sRaw ($P < 0.001$) were observed, regardless of protocol group or PEEP. Conversely, the increases in specific respiratory tissue parameters (sG and sH, $P < 0.001$ for both) by *day 50* were associated with significant PEEP dependence ($P < 0.001$ for both) in both protocol groups (Fig. 2).

Figure 3 depicts the changes in $P_{driving}$ and respiratory mechanical parameters during the 6-h ventilation with PCV or PVV. Although Raw increased significantly with time ($P < 0.001$), the ventilation mode had no significant effect on Raw at any timepoint. Although $P_{driving}$ and the tissue parameters also increased during the 6-h ventilation period in both experimental groups ($P < 0.001$ for all), the deterioration of these parameters was significantly less in Group PVV at *H3* for G, at *H4* for H, and at *H6* for $P_{driving}$ ($P < 0.05$ for all) in comparison to PCV. The mean ventilation rate was not different between the two groups; at *H6*, the rate was 27.5 ± 0.97 and 26.9 ± 0.93 breaths per min in PCV and PVV, respectively.

Parameters obtained by MBW are depicted in Fig. 4, at the beginning (*H0*) and at the end (*H6*) of the 6-h ventilation period. There was no difference between the protocol groups at *H0* for EELV or LCI. However, after 6 h of ventilation, the PCV group exhibited a significant decrease in EELV and increase in LCI that was not present in the PVV group ($P < 0.01$ for both).

Gas exchange parameters reflecting lung oxygenation (Pa_{O_2}/FI_{O_2}) and intrapulmonary shunt fraction (Qs/Qt) are

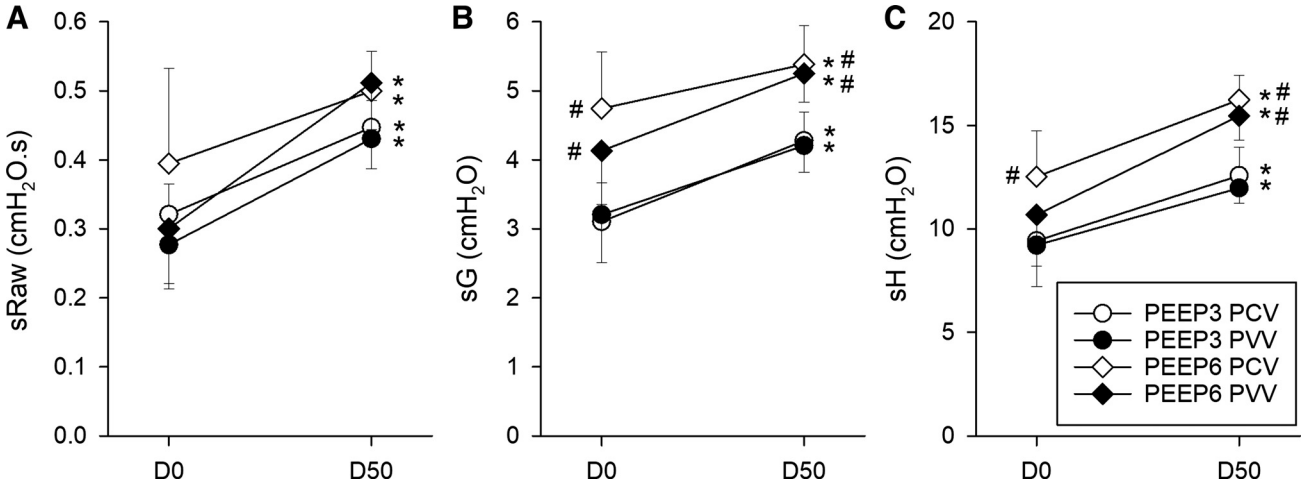

Figure 2. Absolute values of specific airway resistance (sRaw = Raw · EELV; *A*), specific tissue damping (sG = G · EELV; *B*), and specific elastance (sH = H · EELV; *C*) on *day 0* (*D0*) and *day 50* (*D50*) in the two protocol groups (empty symbols: pressure-controlled ventilation, PCV; filled symbols: physiological variable ventilation, PVV) at two PEEP levels (circles: 3 cmH_2O; diamonds: 6 cmH_2O) as mean and 95% confidence interval. *$P < 0.05$ vs. *D0* within a group at the same PEEP; #$P < 0.05$ vs. PEEP 3 cmH_2O in the same group on the same day. EELV, end-expiratory lung volume; G, tissue damping; H, tissue elastance; PEEP, positive end-expiratory pressure; Raw, resistance; sG, specific tissue damping; sH, specific tissue elastance; sRaw, specific resistance.

Downloaded from journals.physiology.org/journal/jappl at Univ De Geneve (129.194.001.044) on November 15, 2022.

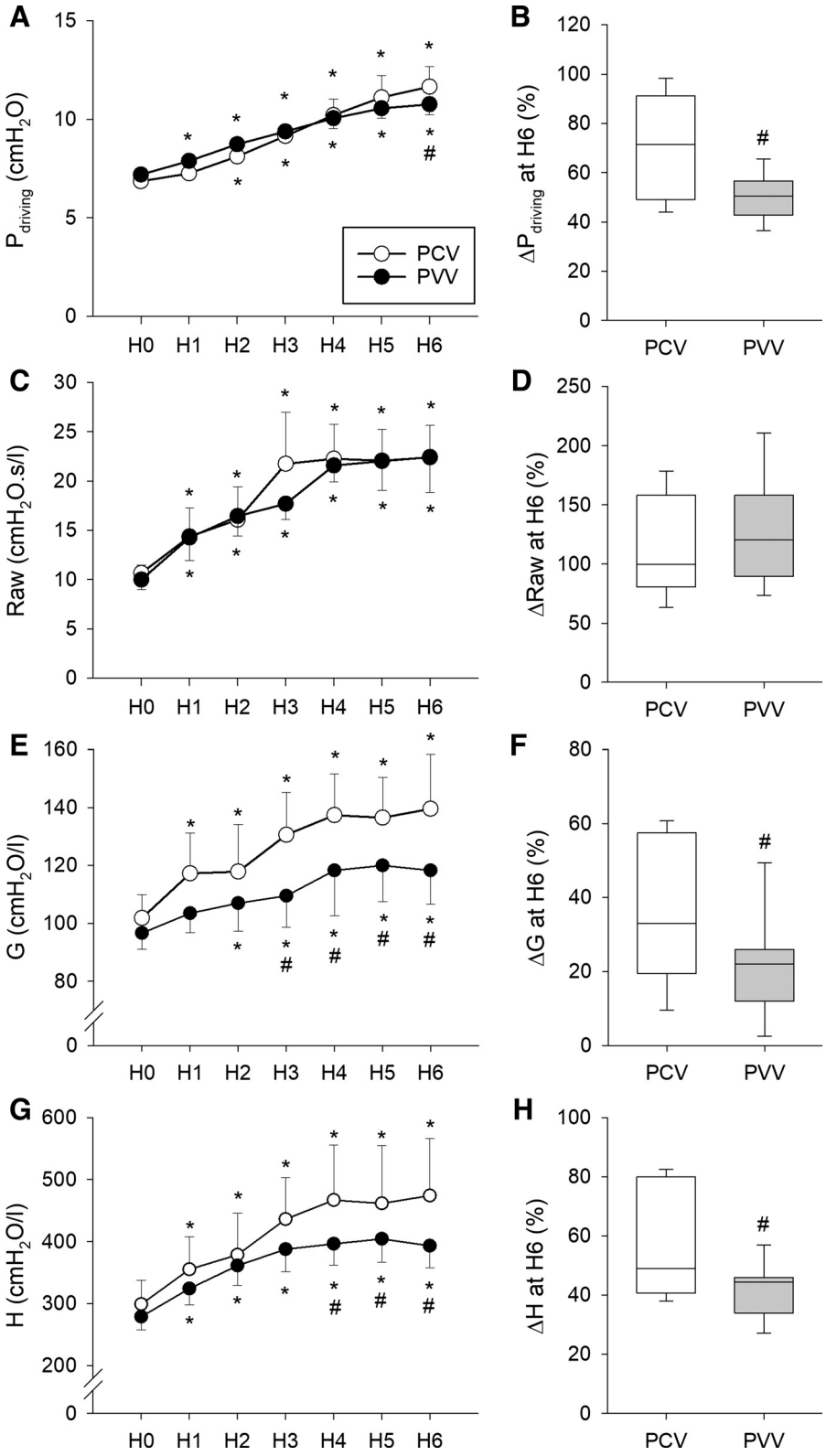

Figure 3. Absolute values of driving pressure ($P_{driving}$; *A*), airway resistance (Raw; *C*), tissue damping (G; *E*), and tissue elastance (H; *G*) during the 6-h ventilation period (*left*) as means and 95% confidence intervals, and their relative changes from *H0* to *H6* as box plots (*right*; *B*, *D*, *F*, *H*) in the group under pressure-controlled ventilation (PCV, empty symbols) and under physiological variable ventilation (PVV, filled symbols). Boxes and whiskers represent the median, interquartile range, and 10th and 90th percentiles, respectively. $*P < 0.05$ vs. *H0* within a group; $\#P < 0.05$ vs. Group PCV.

depicted in Fig. 5. Prolonged mechanical ventilation led to a significant deterioration in both Pa_{O_2}/FI_{O_2} and Qs/Qt in Group PCV ($P < 0.002$ for both). Conversely, the deterioration of both Pa_{O_2}/FI_{O_2} and Qs/Qt was prevented by the application of PVV. After 6 h of ventilation, Pa_{O_2}/FI_{O_2} was significantly higher whereas Qs/Qt was significantly lower in Group PVV compared to Group PCV ($P < 0.05$ for both).

Downloaded from journals.physiology.org/journal/jappl at Univ De Geneve (129.194.001.044) on November 15, 2022.

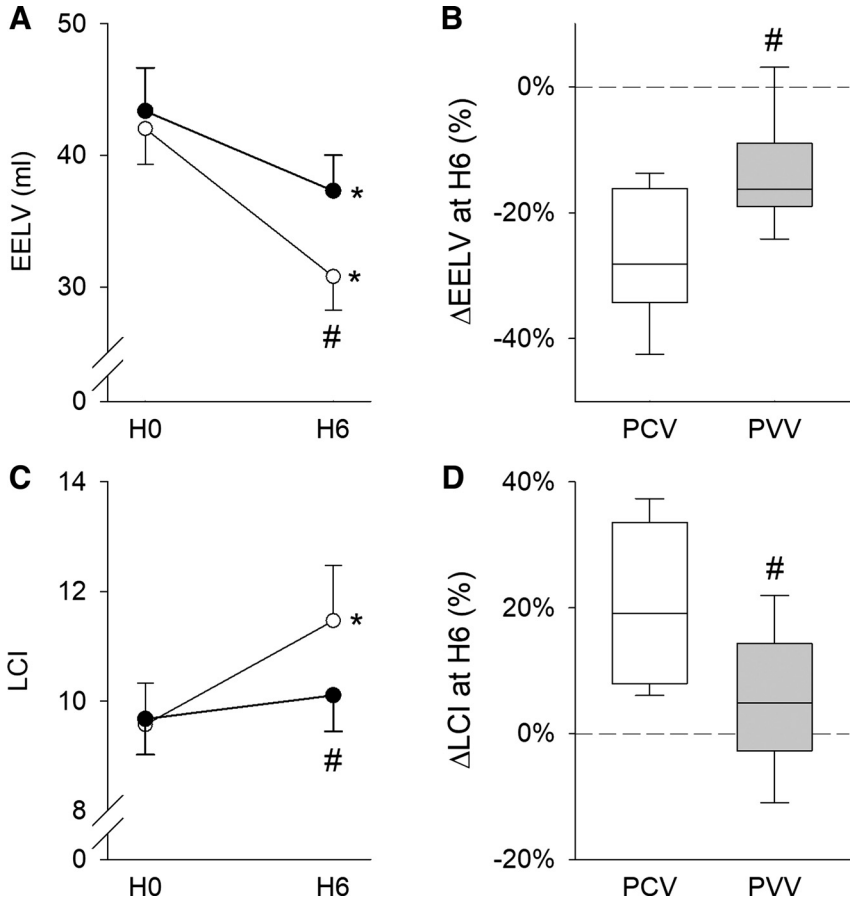

Figure 4. Absolute values of end-expiratory lung volume (EELV; *A*) and lung clearance index (LCI; *C*) during the 6-h ventilation period as mean and 95% confidence interval (*left*) and their relative changes from *H0* to *H6* as box plots (*right*; *B* and *D*) in the group under pressure-controlled ventilation (PCV, empty symbols) and under physiological variable ventilation (PVV, filled symbols). Boxes and whiskers represent the median, interquartile range, and 10th and 90th percentiles, respectively. $*P < 0.05$ vs. *H0* within a group; $\#P < 0.05$ vs. Group PCV.

Histological assessment is represented in Fig. 6. There was no evidence for a statistical difference between the ventilation modes in the overall lung injury score nor in any of its components. Aspects of tissue fibrosis as well as thickening of the alveolar walls and interstitial polymorphonuclear cell infiltration were observed in both experimental groups. Concerning the BALF cell content, no differences were observed between the experimental groups in the total or differential cell count [298.3 (154.2) versus 222.9 (123.6) cells $\times$ 10^4/mL in the PCV and PVV groups, respectively].

DISCUSSION

The comparison of the effects of PVV to conventional PCV revealed the benefits of adding tidal variability onto a monotonous signal during prolonged ventilation. These advantages were manifested in the prevention of deterioration in respiratory tissue mechanics, lung volume loss, development of ventilation heterogeneities, and decline in gas exchange.

We adopted an animal model of pulmonary fibrosis based on the intratracheal nebulization of bleomycin. This model has been validated in multiple species, including mice (19), rats (37), and rabbits (18) and is considered to be the "best-characterized" model of human idiopathic pulmonary fibrosis (21). Although gas exchange abnormalities are mainly present in the acute phase of the disease, that is, 1–7 days following the administration of bleomycin, the morphological characteristics of the chronic stage of lung fibrosis emerge three weeks after endotracheal induction and persist for 3–6 mo (19, 38). Indeed, the study subjects exhibited significant deterioration in the specific airway and respiratory tissue parameters (Fig. 2), which reflect the intrinsic mechanical properties of these compartments. This finding is in agreement with previous results obtained by forced oscillations (39–41) and confirms the development of a pulmonary fibrosis. This organ-level mechanical abnormality originates from the fibrotic remodeling of lung tissue as demonstrated by the histological findings (Fig. 6). The fibrotic transformation induced by bleomycin had no effect on the PEEP-dependence of the specific respiratory mechanical parameters. The lack of effect of PEEP on sRaw remained after bleomycin treatment, which agrees with previous findings demonstrating that sRaw does not depend on lung volume (42). The PEEP dependence of sG and sH on *day 0* and *day 50* can be attributed to the overdistension of respiratory tissues, which thereby increases their dissipative properties and stiffness (43).

The 6-h conventional pressure-controlled mechanical ventilation induced progressive deterioration in airway and tissue mechanics, decrease in lung volume, increase in ventilation heterogeneity, and decline in gas exchange. Contrary to the findings obtained with healthy rabbits under identical experimental conditions (6), the elevations in the mechanical parameters reflecting the flow resistance of the airways

Downloaded from journals.physiology.org/journal/jappl at Univ De Geneve (129.194.001.044) on November 15, 2022.

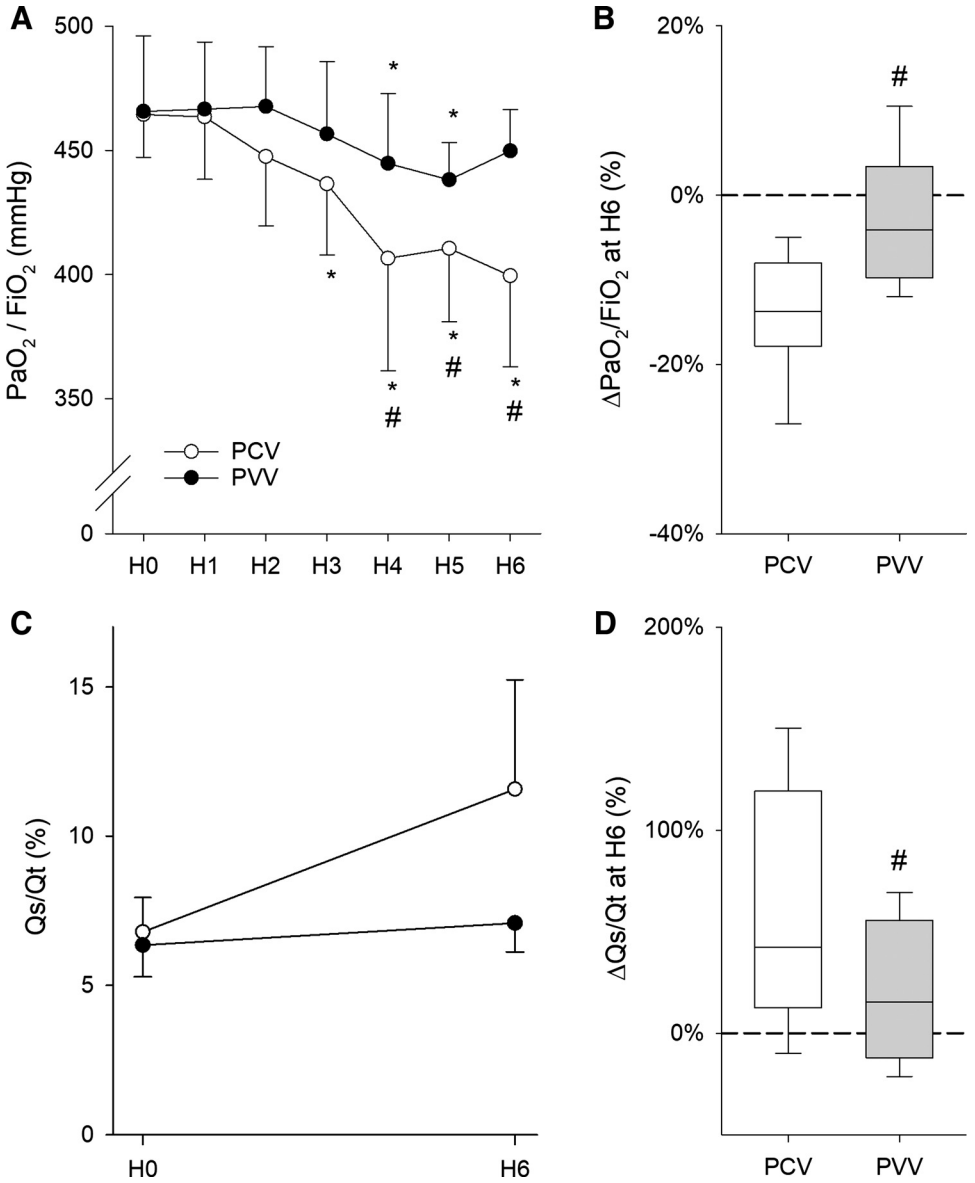

Figure 5. Absolute values of Pa_{O_2}/FI_{O_2} (*A*) and the intrapulmonary shunt fraction (Qs/Qt; *C*) during the 6-h ventilation period as mean and 95% confidence interval (*left*) and their relative changes from *H0* to *H6* as box plots (*right*; *B* and *D*) in the group under pressure-controlled ventilation (PCV, empty symbols) and under physiological variable ventilation (PVV, filled symbols). Boxes and whiskers represent the median, interquartile range, and 10th and 90th percentiles, respectively. $*P < 0.05$ vs. *H0* within a group; $\#P < 0.05$ vs. Group PCV.

and dissipative and elastic properties of the respiratory tissues appeared earlier (*H1*) and were more pronounced. Peribronchial and interstitial inflammation leading to the increased susceptibility of conducting airways to constriction may explain the marked elevations in Raw during the 6-h ventilation period (44), whereas augmented atelectasis development may be responsible for the deterioration of respiratory tissue mechanical parameters. These results are in accordance with the increased risk of ventilation-induced lung injury in the presence of interstitial lung diseases (23).

The most remarkable finding of the present study is the ability of PVV to prevent the deleterious effects of prolonged mechanical ventilation in the lung periphery. The comparable protective effects of PVV on G and H suggest that the introduction of variability in volume and frequency exerts its benefit by preventing derecruitment in the lung peripheral airways and alveolar units. This finding for tissue mechanics is confirmed by the smaller degree of EELV loss (Fig. 4). Furthermore, PVV inhibited the development of ventilation heterogeneities, as evidenced by the lack of increase in LCI after 6 h of mechanical ventilation. As a result of the maintained lung aeration with PVV as opposed to PCV, significantly less deterioration was observed in the parameters reflecting lung oxygenation and ventilation-perfusion matching (Fig. 5). Regarding the mechanism responsible for the maintained lung aeration and gas exchange in PVV, it seems likely that the occasional inspirations with higher V_T led to the recruitment of large lung regions due to avalanche-like airway reopening phenomena (45, 46). Furthermore, the variability in respiratory rate most probably contributes to this recruitment effect, since alveolar units with a wider range of time constants are reopened due to the varying inspiratory times (47). In contrast to a previous study with a rat model of emphysema that demonstrated improvement in ventilation distribution without an increase in EELV (48), our results evidenced the preservation

Downloaded from journals.physiology.org/journal/jappl at Univ De Geneve (129.194.001.044) on November 15, 2022.

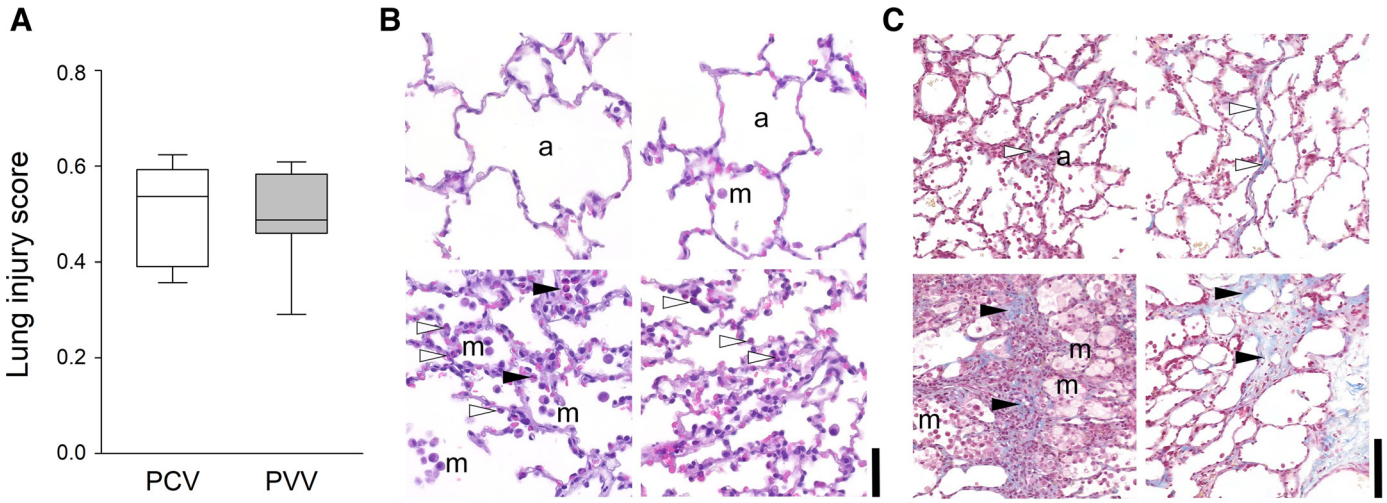

Figure 6. Histological features observed in the lungs after bleomycin-induced pulmonary injury and 6 h of mechanical ventilation. *A*: overall lung injury score according to ref. (34) in the group under pressure-controlled ventilation (PCV, empty bar) and under physiological variable ventilation (PVV, filled bar). Boxes and whiskers represent the median, interquartile range, and 10th and 90th percentiles, respectively. *B*: animals from both experimental groups show variable areas of regular alveolar spaces (a) with thin walls and occasional alveolar macrophages (m), similar to normal lung. These are interspersed with areas displaying small or collapsed alveoli, with irregular alveolar spaces, numerous alveolar macrophages, and thickened alveolar walls with intramural/interstitial polymorphonuclear cells, i.e., heterophils, corresponding to human neutrophils (black arrowhead), also occasionally present inside the alveoli (white arrowhead). Hematoxylin and eosin, original magnification ×400, bar, 20 μm. *C*: lung tissue with multifocal areas of thickened septa (white arrowhead) and, more rarely, of fibrotic masses and fibrotic collapsed alveoli (black arrowhead), associated with aggregates of alveolar macrophages. Masson's trichrome, original magnification ×200, bar is 50 μm.

of lung volume with PVV along with the maintained ventilation homogeneity.

The benefit of PVV in a model of pulmonary fibrosis is in accordance with previous findings demonstrating that the superposition of variability onto conventional mechanical ventilation improves lung compliance (4, 10, 15, 49) and leads to improved recruitment of closed alveoli and subsequent improvement in gas exchange (4, 10, 15) as well as reduced histological damage (17). Recently our research group proposed the concept of physiologically variable ventilation as an advancement over the mathematically derived variable pattern (6, 31) and over the biologically variable ventilation (50). The PVV is based on the application of a prerecorded spontaneous breathing pattern, with naturally varying V_T and respiratory rate, from awake animals, and differs from the biologically variable ventilation proposed by the pioneer work of Mutch and colleagues in that it results in varying frequency-tidal volume product (51). In addition to its advantage for healthy (6), asthma (13), COPD (14), and ARDS lungs (31), the results of the present study also evidenced the particular benefit of this approach compared to the conventional pressure-controlled mode in a model of pulmonary fibrosis.

The present study possesses certain limitations and methodological aspects. To comply with the use of minimal number of animals in accordance with the replacement-reduction-refinement principle, no control group receiving sham treatment on *day 0* was included. Although changes in respiratory mechanical parameters were biased by lung growth, the efficiency of bleomycin treatment could be estimated from the specific mechanical parameters and histological analyses (Figs. 2 and 6). Furthermore, we were able to compare changes in respiratory parameters measured during the 6-h ventilation to data obtained from previous studies with identical experimental protocols. Although the experimental model used in the present work may lack some of the clinical features of interstitial lung diseases, it mimics histological and mechanical features resembling the human pathology. Another limitation may be related to the relatively short ventilation protocol, which precluded the development of severe lung injury. However, the benefit of PVV by preventing alveolar derecruitment was apparent in this time frame, and it can be anticipated that this benefit persists for an even longer period. A methodological aspect of the present study is the use of a PVV pattern previously recorded in a healthy rabbit to ventilate rabbits in a pathological condition. Although the application of a disease-specific or even individualized respiratory pattern may have yielded greater benefit, the general PVV pattern is more feasible due to its reproducibility and demonstrated significant benefits in the setting of pulmonary fibrosis.

In conclusion, we demonstrated that, in a bleomycin-induced model of pulmonary fibrosis, the application of physiological variability during prolonged mechanical ventilation maintains gas exchange by preventing atelectasis development, as compared with the conventional pressure-controlled mode. This finding suggests that the increased risk for ventilator-induced lung injury in the presence of pulmonary fibrosis can be mitigated by keeping the lung open with a PVV pattern, which does not require an increase in $P_{driving}$.

GRANTS

Financial support was provided from the Swiss National Science Foundation grant 32003B_169334 attributed to Prof. Walid Habre.

DISCLOSURES

No conflicts of interest, financial or otherwise, are declared by the authors.

Downloaded from journals.physiology.org/journal/jappl at Univ De Geneve (129.194.001.044) on November 15, 2022.

AUTHOR CONTRIBUTIONS

A.D.S.R., F.P., W.H., and A.L.B. conceived and designed research; A.D.S.R. and A.L.B. performed experiments; A.D.S.R., F.P., T.C., W.H., and A.L.B. analyzed data; A.D.S.R., F.P., T.C., W.H., and A.L.B. interpreted results of experiments; A.D.S.R., F.P., T.C., W.H., and A.L.B. prepared figures; A.D.S.R., F.P., W.H., and A.L.B. drafted manuscript; A.D.S.R., F.P., T.C., W.H., and A.L.B. edited and revised manuscript; A.D.S.R., F.P., T.C., W.H., and A.L.B. approved final version of manuscript.

REFERENCES

1. **Mutch WA**, **Eschun GM**, **Kowalski SE**, **Graham MR**, **Girling LG**, **Lefevre GR.** Biologically variable ventilation prevents deterioration of gas exchange during prolonged anaesthesia. *Br J Anaesth* 84: 197–203, 2000. doi:10.1093/oxfordjournals.bja.a013403.
2. **Mutch WA**, **Harms S**, **Ruth Graham M**, **Kowalski SE**, **Girling LG**, **Lefevre GR.** Biologically variable or naturally noisy mechanical ventilation recruits atelectatic lung. *Am J Respir Crit Care Med* 162: 319–323, 2000. doi:10.1164/ajrccm.162.1.9903120.
3. **Boker A**, **Graham MR**, **Walley KR**, **McManus BM**, **Girling LG**, **Walker E**, **Lefevre GR**, **Wa M.** Improved arterial oxygenation with biologically variable or fractal ventilation using low tidal volumes in a porcine model of acute respiratory distress syndrome. *Am J Respir Crit Care Med* 165: 456–462, 2002. doi:10.1164/ajrccm.165.4.2108006.
4. **Arold SP**, **Mora R**, **Lutchen KR**, **Ingenito EP**, **Suki B.** Variable tidal volume ventilation improves lung mechanics and gas exchange in a rodent model of acute lung injury. *Am J Respir Crit Care Med* 165: 366–371, 2002. doi:10.1164/ajrccm.165.3.2010155.
5. **Thammanomai A**, **Hamakawa H**, **Bartolák-Suki E**, **Suki B.** Combined effects of ventilation mode and positive end-expiratory pressure on mechanics, gas exchange and the epithelium in mice with acute lung injury. *PloS One* 8: e53934, 2013. doi:10.1371/journal.pone.0053934.
6. **Walesa M**, **Bayat S**, **Albu G**, **Baudat A**, **Petak F**, **Habre W.** Comparison between neurally-assisted, controlled, and physiologically variable ventilation in healthy rabbits. *Br J Anaesth* 121: 918–927, 2018. doi:10.1016/j.bja.2018.01.020.
7. **Fodor GH**, **Petak F**, **Erces D**, **Balogh AL**, **Babik B.** Lung mechanical changes following bronchoaspiration in a porcine model: differentiation of direct and indirect mechanisms. *Respir Physiol Neurobiol* 199: 41–49, 2014. doi:10.1016/j.resp.2014.05.001.
8. **Thammanomai A**, **Hueser LE**, **Majumdar A**, **Bartolák-Suki E**, **Suki B.** Design of a new variable-ventilation method optimized for lung recruitment in mice. *J Appl Physiol (1985)* 104: 1329–1340, 2008. [Erratum in *J Appl Physiol* 104: 1856, 2008]. doi:10.1152/japplphysiol.01002.2007.
9. **Arold SP**, **Bartolák-Suki E**, **Suki B.** Variable stretch pattern enhances surfactant secretion in alveolar type II cells in culture. *Am J Physiol Lung Cell Mol Physiol* 296: L574–L581, 2009. doi:10.1152/ajplung.90454.2008.
10. **Arold SP**, **Suki B**, **Alencar AM**, **Lutchen KR**, **Ingenito EP.** Variable ventilation induces endogenous surfactant release in normal guinea pigs. *Am J Physiol Lung Cell Mol Physiol* 285: L370– L375, 2003. doi:10.1152/ajplung.00036.2003.
11. **Bartolák-Suki E**, **Noble PB**, **Bou Jawde S**, **Pillow JJ**, **Suki B.** Optimization of variable ventilation for physiology, immune response and surfactant enhancement in preterm lambs. *Front Physiol* 8: 425, 2017. doi:10.3389/fphys.2017.00425.
12. **Kiss T**, **Silva PL**, **Huhle R**, **Moraes L**, **Santos RS**, **Felix NS**, **Santos CL**, **Morales MM**, **Capelozzi VL**, **Kasper M**, **Pelosi P**, **Gama de Abreu M**, **Rocco PR.** Comparison of different degrees of variability in tidal volume to prevent deterioration of respiratory system elastance in experimental acute lung inflammation. *Br J Anaesth* 116: 708–715, 2016. doi:10.1093/bja/aew093.
13. **Dos Santos Rocha A**, **Südy R**, **Peták F**, **Habre W.** Physiologically variable ventilation in a rabbit model of asthma exacerbation. *Br J Anaesth* 125: 1107–1116, 2020. doi:10.1016/j.bja.2020.08.059.
14. **Santos Rocha AD**, **Südy R**, **Bizzotto D**, **Kassai M**, **Carvalho T**, **Dellacà RL**, **Peták F**, **Habre W.** Benefit of physiologically variable over pressure-controlled ventilation in a model of chronic obstructive pulmonary disease: a randomized study. *Front Physiol* 11: 625777, 2020. doi:10.3389/fphys.2020.625777.
15. **Bellardine CL**, **Hoffman AM**, **Tsai L**, **Ingenito EP**, **Arold SP**, **Lutchen KR**, **Suki B.** Comparison of variable and conventional ventilation in a sheep saline lavage lung injury model. *Crit Care Med* 34: 439–445, 2006. doi:10.1097/01.ccm.0000196208.01682.87.
16. **Dos Santos Rocha A**, **Fodor GH**, **Kassai M**, **Degrugilliers L**, **Bayat S**, **Petak F**, **Habre W.** Physiologically variable ventilation reduces regional lung inflammation in a pediatric model of acute respiratory distress syndrome. *Respir Res* 21: 288, 2020. doi:10.1186/s12931-020-01559-x.
17. **Spieth PM**, **Carvalho AR**, **Pelosi P**, **Hoehn C**, **Meissner C**, **Kasper M**, **Hübler M**, **von Neindorff M**, **Dassow C**, **Barrenschee M**, **Uhlig S**, **Koch T**, **de Abreu MG.** Variable tidal volumes improve lung protective ventilation strategies in experimental lung injury. *Am J Respir Crit Care Med* 179: 684–693, 2009. doi:10.1164/rccm.200806-975OC.
18. **Günther A**, **Lübke N**, **Ermert M**, **Schermuly RT**, **Weissmann N**, **Breithecker A**, **Markart P**, **Ruppert C**, **Quanz K**, **Ermert L**, **Grimminger F**, **Seeger W.** Prevention of bleomycin-induced lung fibrosis by aerosolization of heparin or urokinase in rabbits. *Am J Respir Crit Care Med* 168: 1358–1365, 2003. doi:10.1164/rccm.2201082.
19. **Moore BB**, **Hogaboam CM.** Murine models of pulmonary fibrosis. *Am J Physiol Lung Cell Mol Physiol* 294: L152–L160, 2008. doi:10.1152/ajplung.00313.2007.
20. **Tashiro J**, **Rubio GA**, **Limper AH**, **Williams K**, **Elliot SJ**, **Ninou I**, **Aidinis V**, **Tzouvelekis A**, **Glassberg MK.** Exploring animal models that resemble idiopathic pulmonary fibrosis. *Front Med (Lausanne)* 4: 118, 2017. doi:10.3389/fmed.2017.00118.
21. **Jenkins RG**, **Moore BB**, **Chambers RC**, **Eickelberg O**, **Konigshoff M**, **Kolb M**, **Laurent GJ**, **Nanthakumar CB**, **Olman MA**, **Pardo A**, **Selman M**, **Sheppard D**, **Sime PJ**, **Tager AM**, **Tatler AL**, **Thannickal VJ**, **White ES**; **ATS Assembly on Respiratory Cell and Molecular Biology.** An Official American Thoracic Society Workshop Report: use of animal models for the preclinical assessment of potential therapies for pulmonary fibrosis. *Am J Respir Cell Mol Biol* 56: 667–679, 2017. doi:10.1165/rcmb.2017-0096ST.
22. **Marchioni A**, **Tonelli R**, **Rossi G**, **Spagnolo P**, **Luppi F**, **Cerri S**, **Cocconcelli E**, **Pellegrino MR**, **Fantini R**, **Tabbì L**, **Castaniere I**, **Ball L**, **Malbrain M**, **Pelosi P**, **Clini E.** Ventilatory support and mechanical properties of the fibrotic lung acting as a "squishy ball. *Ann Intensive Care* 10: 13, 2020. doi:10.1186/s13613-020-0632-6.
23. **Ryerson CJ**, **Cottin V**, **Brown KK**, **Collard HR.** Acute exacerbation of idiopathic pulmonary fibrosis: shifting the paradigm. *Eur Respir J* 46: 512–520, 2015. doi:10.1183/13993003.00419-2015.
24. **Albu G**, **Wallin M**, **Hallbäck M**, **Emtell P**, **Wolf A**, **Lönnqvist PA**, **Göthberg S**, **Peták F**, **Habre W.** Comparison of static end-expiratory and effective lung volumes for gas exchange in healthy and surfactant-depleted lungs. *Anesthesiology* 119: 101–110, 2013. doi:10.1097/ALN.0b013e3182923c40.
25. **Horsley A.** Lung clearance index in the assessment of airways disease. *Respir Med* 103: 793–799, 2009. doi:10.1016/j.rmed.2009.01.025.
26. **Becklake MR.** A new index of the intrapulmonary mixture of inspired air. *Thorax* 7: 111–116, 1952. doi:10.1136/thx.7.1.111.
27. **Bayat S**, **Strengell S**, **Porra L**, **Janosi TZ**, **Petak F**, **Suhonen H**, **Suortti P**, **Hantos Z**, **Sovijärvi AR**, **Habre W.** Methacholine and ovalbumin challenges assessed by forced oscillations and synchrotron lung imaging. *Am J Respir Crit Care Med* 180: 296–303, 2009. doi:10.1164/rccm.200808-1211OC.
28. **Hantos Z**, **Daróczy B**, **Suki B**, **Nagy S**, **Fredberg JJ.** Input impedance and peripheral inhomogeneity of dog lungs. *J Appl Physiol (1985)* 72: 168–178, 1992. doi:10.1152/jappl.1992.72.1.168.
29. **Peták F**, **Hantos Z**, **Adamicza Á**, **Asztalos T**, **Sly PD.** Methacholine-induced bronchoconstriction in rats: effects of intravenous vs. aerosol delivery. *J Appl Physiol* 82: 1479–1487, 1997. doi:10.1152/jappl.1997.82.5.1479.
30. **Berggren SM.** *The Oxygen Deficit of Arterial Blood Caused by Non-Ventilating Parts of the Lung*. Stockholm: Norstedt, 1942, vol. 4, p. 1–92.
31. **Fodor GH**, **Bayat S**, **Albu G**, **Lin N**, **Baudat A**, **Danis J**, **Petak F**, **Habre W.** Variable ventilation is equally effective as conventional pressure control ventilation for optimizing lung function in a rabbit

Downloaded from journals.physiology.org/journal/jappl at Univ De Geneve (129.194.001.044) on November 15, 2022.

model of ARDS. *Front Physiol* 10: 803, 2019. doi:10.3389/fphys.2019.00803.
32. **Ashcroft T**, **Simpson JM**, **Timbrell V.** Simple method of estimating severity of pulmonary fibrosis on a numerical scale. *J Clin Pathol* 41: 467–470, 1988. doi:10.1136/jcp.41.4.467.
33. **Hübner RH**, **Gitter W**, **El Mokhtari NE**, **Mathiak M**, **Both M**, **Bolte H**, **Freitag-Wolf S**, **Bewig B.** Standardized quantification of pulmonary fibrosis in histological samples. *Biotechniques* 44: 507–507, 2008. doi:10.2144/000112729.
34. **Matute-Bello G**, **Downey G**, **Moore BB**, **Groshong SD**, **Matthay MA**, **Slutsky AS**, **Kuebler WM**; **Acute Lung Injury in Animals Study Group.** An official American Thoracic Society workshop report: features and measurements of experimental acute lung injury in animals. *Am J Respir Cell Mol Biol* 44: 725–738, 2011. doi:10.1165/rcmb.2009-0210ST.
35. **Bates D**, **Mächler M**, **Bolker B**, **Walker S.** Fitting linear mixed-effects models using lme4. *J Stat Soft* 67: 48, 2015. doi:10.18637/jss.v067.i01.
36. **Lenth RV.** Least-squares means: The RPackage lsmeans. *J Stat Softw* 69: 1–33, 2016. doi:10.18637/jss.v069.i01.
37. **Thrall RS**, **McCormick JR**, **Jack RM**, **McReynolds RA**, **Ward PA.** Bleomycin-induced pulmonary fibrosis in the rat: inhibition by indomethacin. *Am J Pathol* 95: 117–130, 1979.
38. **Limjunyawong N**, **Mitzner W**, **Horton MR.** A mouse model of chronic idiopathic pulmonary fibrosis. *Physiol Rep* 2: e00249, 2014. doi:10.1002/phy2.249.
39. **Headley L**, **Bi W**, **Wilson C**, **Collum SD**, **Chavez M**, **Darwiche T**, **Mertens TCJ**, **Hernandez AM**, **Siddiqui SR**, **Rosenbaum S**, **Johnston RA**, **Karmouty-Quintana H.** Low-dose administration of bleomycin leads to early alterations in lung mechanics. *Exp Physiol* 103: 1692–1703, 2018. doi:10.1113/EP087322.
40. **Devos FC**, **Maaske A**, **Robichaud A**, **Pollaris L**, **Seys S**, **Lopez CA**, **Verbeken E**, **Tenbusch M**, **Lories R**, **Nemery B**, **Hoet PH**, **Vanoirbeek JA.** Forced expiration measurements in mouse models of obstructive and restrictive lung diseases. *Respir Res* 18: 123, 2017. doi:10.1186/s12931-017-0610-1.
41. **Manali ED**, **Moschos C**, **Triantafillidou C**, **Kotanidou A**, **Psallidas I**, **Karabela SP**, **Roussos C**, **Papiris S**, **Armaganidis A**, **Stathopoulos GT**, **Maniatis NA.** Static and dynamic mechanics of the murine lung after intratracheal bleomycin. *BMC Pulm Med* 11: 33, 2011. doi:10.1186/1471-2466-11-33.
42. **Briscoe WA**, **Dubois AB.** The relationship between airway resistance, airway conductance and lung volume in subjects of different age and body size. *J Clin Invest* 37: 1279–1285, 1958. doi:10.1172/JCI103715.
43. **Pelosi P**, **Cereda M**, **Foti G**, **Giacomini M**, **Pesenti A.** Alterations of lung and chest wall mechanics in patients with acute lung injury: effects of positive end-expiratory pressure. *Am J Respir Crit Care Med* 152: 531–537, 1995. doi:10.1164/ajrccm.152.2.7633703.
44. **Polosukhin VV**, **Degryse AL**, **Newcomb DC**, **Jones BR**, **Ware LB**, **Lee JW**, **Loyd JE**, **Blackwell TS**, **Lawson WE.** Intratracheal bleomycin causes airway remodeling and airflow obstruction in mice. *Exp Lung Res* 38: 135–146, 2012. doi:10.3109/01902148.2012.658595.
45. **Suki B**, **Alencar AM**, **Sujeer MK**, **Lutchen KR**, **Collins JJ**, **Andrade JS Jr**, **Ingenito EP**, **Zapperi S**, **Stanley HE.** Life-support system benefits from noise. *Nature* 393: 127–128, 1998. doi:10.1038/30130.
46. **Suki B**, **Barabási AL**, **Hantos Z**, **Peták F**, **Stanley HE.** Avalanches and power-law behaviour in lung inflation. *Nature* 368: 615–618, 1994. doi:10.1038/368615a0.
47. **Ma B**, **Suki B**, **Bates JH.** Effects of recruitment/derecruitment dynamics on the efficacy of variable ventilation. *J Appl Physiol (1985)* 110: 1319–1326, 2011. doi:10.1152/japplphysiol.01364.2010.
48. **Henriques I**, **Padilha GA**, **Huhle R**, **Wierzchon C**, **Miranda PJ**, **Ramos IP**, **Rocha N**, **Cruz FF**, **Santos RS**, **de Oliveira MV**, **Souza SA**, **Goldenberg RC**, **Luiz RR**, **Pelosi P**, **de Abreu MG**, **Silva PL**, **Rocco PR.** Comparison between variable and conventional volume-controlled ventilation on cardiorespiratory parameters in experimental emphysema. *Front Physiol* 7: 277, 2016. doi:10.3389/fphys.2016.00277.
49. **Berry CA**, **Suki B**, **Polglase GR**, **Pillow JJ.** Variable ventilation enhances ventilation without exacerbating injury in preterm lambs with respiratory distress syndrome. *Pediatr Res* 72: 384–392, 2012. doi:10.1038/pr.2012.97.
50. **Lefevre GR**, **Kowalski SE**, **Girling LG**, **Thiessen DB**, **Mutch WA.** Improved arterial oxygenation after oleic acid lung injury in the pig using a computer-controlled mechanical ventilator. *Am J Respir Crit Care Med* 154: 1567–1572, 1996. doi:10.1164/ajrccm.154.5.8912782.
51. **Dos Santos Rocha A**, **Südy R**, **Peták F**, **Habre W.** Physiologically variable ventilation and severe asthma. Response to Br J Anaesth 2020; 126, e214. *Br J Anaesth* 127: e93–e94, 2021. doi:10.1016/j.bja.2021.05.029.

Downloaded from journals.physiology.org/journal/jappl at Univ De Geneve (129.194.001.044) on November 15, 2022.